Fibers and Polymers 2007, Vol.8, No.4, 377-385

Polyurethane Smart Fiber with Shape Memory Function: Experimental Characterization and Constitutive Modelling

Seok Jin Hong, Woong-Ryeol Yu*, Ji Ho Youk[1], and Yang Rae Cho[2]

Department of Materials Science and Engineering, Seoul National University, Seoul 151-742, Korea
[1]Department of Advanced Fiber Engineering, Division of Nano-Systems, Inha University, Incheon 402-751, Korea
[2]Chemex Ulsan R&D Center, Hosung Chemex Co., Ulsan 689-821, Korea
(Received March 21, 2007; Revised May 28, 2007; Accepted June 9, 2007)

Abstract: Segmented polyurethane (PU) polymers are known to have shape memory function, i.e., when they reach certain temperatures, they deform into the memorized shape from any temporary one. In the present study, PU polymers were spun into fibers using the conventional extrusion process to investigate the feasibility of producing smart fibers with shape memory function. The shape memory polymers (SMPs) and their spun fibers were characterized using DSC, DMTA, and tensile test. In particular, the thermo-mechanical deformation behavior, which enables to evaluate the shape memory performance of the SMPs, was characterized using DMTA. Then, the linear viscoelastic theory was utilized for mathematical modelling of the thermo-mechanical behavior of the SMPs. For the shape memory fibers, the large deformation characteristics were also investigated using the thermo-mechanical test, necessitating the development of nonlinear viscoelastic theory to formulate a constitutive equation and to provide an effective tool for designing smart textile structure.

Keywords: Shape memory polymer, Polyurethane, Smart fiber, Viscoelastic theory

Introduction

There have been various attempts made to develop smart materials which are responsive to certain stimuli such as temperature, electric current, acidity, etc. Temperature sensitive materials are materials that can change their physical shape, e.g., from strained shapes to an unstrained shape, as they reach specific temperatures. Since the unstrained shape is referred to the memorized (or permanent) shape to which any temporary shapes return upon heating, such materials are called shape memory materials, among which shape memory polymers (SMPs) and metal alloys can be exemplified. Many researches [1-3] have been dedicated to develop SMPs due to their good processibility, light weight, low cost, and high recovery strain. In addition, due to their biocompatibility, the SMPs have been applied to biomedical devices with smart function [4,5].

Polyurethanes (PUs) with the segmented structure have been observed to have shape memory property [6-12]. Such PUs are block-copolymers that consist of the soft- and hard-segments, which are incompatible due to an increase in the Gibb's free energy of mixing and thus have a tendency toward the micro-phase separation. The degree of the phase separation is affected by the hydrogen bonding between polymer chains, segmental length, polarity, crystallinity, overall composition, etc. [6,7]. Since the ratio of hard-segment to soft-segment in the molecular mass is an important factor for the micro-phase separation, the shape (or strain) fixity and recovery rates, which are criterions to assess the shape memory performance, are characterized with the ratio [8,11,12].

A typical behavior of SMP is illustrated in Figure 1 [13]. Thermoplastic SMPs can be processed to have a permanent shape using thermo-processes. At higher temperature than the transition temperature (T_{tr}), SMP is mechanically deformed into a temporary shape (stage ① in Figure 1). The temporary shape is now fixed by lowering the temperature (stage ② in Figure 1) and releasing the stress (stage ③ in Figure 1). At this moment, the polymer molecules in SMP also tend to return to the permanent shape without deformation; however since the rigidity in the molecules was increased by lowering the temperature, they can not take up all the deformation, thereby leaving the temporary shape fixed. Here, the strain fixity rate can be defined as the difference in shapes after stage ① and ③, and it can be a criterion to assess the shape memory performance because large strain fixity rate implies better micro-phase separation in SMP. Upon heating the rigidity of polymer chains in the soft-segment decreases, thereby the frozen stress becomes activated such that SMP recovers all the deformation and returns to the permanent shape (stage ④ in Figure 1). Here, the strain recovery rate also can be a criterion to assess the shape memory performance.

As explained above, SMPs are required to have less rigid soft-segment (reversible phase in that it deforms during the fixation process and restore its permanent shape upon heating) and rigid hard-segment (frozen phase). Since the hard-segment acts like net points and remains rigid during the memorizing process (stage ② in Figure 1), both the deformation to the temporary shape and the recovery to the permanent shape are determined by the variation of the rigidity in the soft-segment according to temperature. The transition in the rigidity of polymer molecules is governed by the glass transition temperature (T_g) or the melting temperature (T_m) depending on their ability to crystallize. Various SMPs with different mechanical properties can be developed by controlling the

*Corresponding author: woongryu@snu.ac.kr

transition temperature such as T_g or T_m in the soft-segment, the level of micro-phase separation, and the structure of the hard-segment. Due to the flexible design of the molecular structure, SMPs have been utilized for various applications including biomedical device such as self-deployable stents [4] and self-tightening sutures [5] and smart polymer composites [14-18].

To design smart devices using SMPs effectively, their thermo-mechanical behavior should be characterized. As shown in Figure 1, the characterization can be completed by tracing the whole deformation behavior in the cyclic test. For this purpose a tensile testing machine with a specific control program has been used [2,13]. Frequently the strain fixity and recovery rates only have been measured because the general tensile testers can not trace the cyclic deformation in Figure 1, making it difficult to characterize the transition behavior of SMPs [7-9,14]. In the present study DMTA was utilized to characterize the transition behavior of SMPs, which has not been reported so far to authors' knowledge.

SMPs' application to textiles has been mainly focused on the coated textile, which utilizes a characteristic of SMP, i.e., its gas permeability varies due to the micro-Brownian motion as the temperature changes. There have been few attempts to produce smart fibers from SMPs for textile application. In this study, smart fibers were spun from the linear SMPs using the conventional spinning process with an extruding system and their thermo-mechanical behavior was investigated.

Concerning the constitutive modelling of SMPs, a few reports have been published [19-21]. Linear and nonlinear viscoelastic theories were applied to describe the thermo-mechanical behavior of SMPs [19,20]. Four-elements mechanical unit (spring, dashpot, frictional device) was used to derive a differential constitutive equation. To determine the material properties in the differential constitutive equation, it was assumed that modulus, viscosity, and other parameters are decayed exponentially according to temperature. Liu *et al.* [21] attempted to develop a constitutive equation based on the thermodynamic concepts of entropy and internal energy. Adopting the concept of 'frozen' strain, they demonstrated

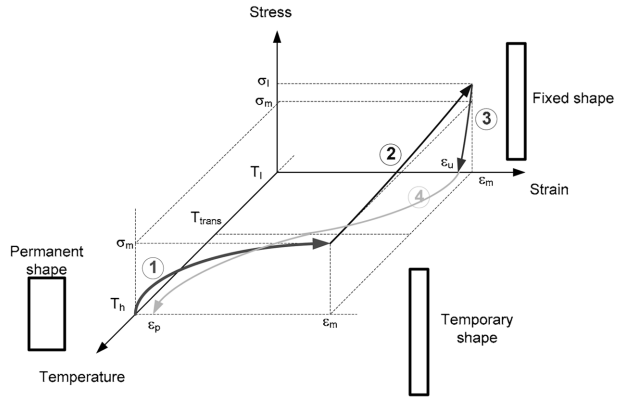

Figure 1. A typical thermo-mechanical behavior of SMP.

the utility of their model by simulating the strain and stress recovery under various flexible constraint levels. The present study adopted the rheological approach using the linear viscoelastic theory as the first trial; however, this study did not rely on the differential constitutive equation, which can be derived by assuming a mechanical analogy unit (see [19,20]). Instead, the relaxation modulus was measured in various temperatures and used to construct the master curve, enabling us to calculate the stress. More detailed results will be provided after discussing experiments for the characterization and melt-spinning of SMP.

Experimental

Materials

There are many SMPs which are responsible to temperature. In this research, two materials were used to investigate the thermo-mechanical behavior of SMP and further to assess the feasibility of utilizing SMP to develop smart fibers with the thermo-responsible function. Both materials used here were PU block copolymers consisting of the hard and soft segments. Sample 'A' material (from Hosung Chemex Co. in Korea) was synthesized by one step process with 4,4'-diphenylmethane diisocyanate (MDI), poly(tetramethylene adipate) (PTMA, Mw=2000) and 1,4-butanediol (BD). The molar ratio for this sample synthesis was 4:1:3 for MDI: PTMA:BD with the hard segment fraction being 38.8 % in weight. Sample 'B' was synthesized by a two-step method, with MDI, poly(e-caprolactone diol) (PCL, Mw=2000), and BD. The molar ratio of the constituents in sample 'B' was also 4:1:3 for MDI:PCL:BD.

Thermal Analysis

The transition temperature of SMP is a temperature that can fix the strain imposed at high temperature by cooling. The transition temperature relies on the molecular arrangement of the soft segments. In the present study, T_m was determined as the transition temperature because the soft segment in both materials can crystallize to an extent. It is clear from Figure 2 that T_m of the soft segment (33.5 °C) can be defined as the transition temperature of sample 'A' SMP, whereas the sample B does not show such sharp transition temperature. This may be due to the low molecular weight of PCL used in this work and relatively high hard-segment fraction because low molecular weight of PCL can not crystallize due to the hindrance by the hard segment when the hard segment fraction is relatively high [22]. A temperature (22.5 °C) was chosen for the transition temperature of the sample 'B' material considering the variation of storage modulus according to temperature.

Spinning of the SMPs

Sample 'A' and 'B' SMPs were spun into fibers using the conventional extrusion process. The screw diameter of the

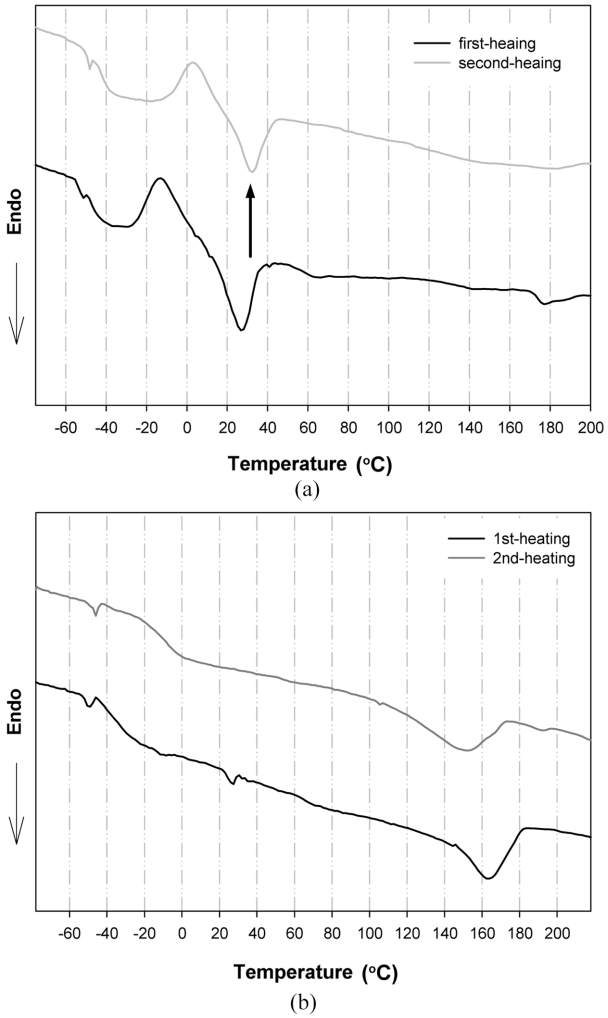

Figure 2. DSC thermodiagrams of (a) sample 'A' SMP and (b) sample 'B' SMP.

Table 1. Spinning conditions of SMPs

Sample code	Temperature (°C)				Winding speed (rpm)	Screw speed (rpm)
	Feeding zone	Zone 2	Zone 3	Die		
A	175	180	185	190	350	14
B	185	190	195	195	350	30

extruder (Microtruder, Randcastle RCP-0500) used in this study was 12.7 mm (0.5 inch) and the output rate was 82 to 983 g per hour (for linear low density polyethylene at minimum speeds of 10 rpm and maximum speeds of 120 rpm). The diameter of the die nozzle was 0.7 mm. Considering rheological properties including the melt flow, the extrusion conditions were set up as shown in Table 1.

Thermo-mechanical Characterization

As shown in Figure 1, the thermo-mechanical test of SMPs consists of four steps; 1) deforming at the higher temperature than the transition one, 2) cooling down to the lower temperature maintaining the strain constant, 3) releasing the stress, and 4) heating up to the high temperature keeping the stress zero. During each testing step, the strain and stress should be recorded to characterize the thermo-mehcanical behaviour of SMPs. General tensile tester equipped with the environmental chamber can be used, however, the full history of the strain and stress may not be recorded without the special control program. In this research, DMTA was utilized by slightly modifying the third step. In the third step, the load should be released continuously, however since the current setup of DMTA does not allow such linear drop, stepwise drops were programmed to simulate the linear drop. Details on experimental condition are listed in Table 2. Two deformation modes, i.e., bending and tensile modes were adopted for the current thermo-mechanical characterization. The bending mode was applied to thin film specimens for small deformation case, whereas melt spun fibers were tested in the tensile mode.

Table 2. Thermo-mechanical test condition of SMPs

	Input	Constraint	Output
1st step	Strain	Strain rate: 5 %/min, Temp: T_{tr}+20 °C	stress
2nd step	Cooling	Strain fixed: Temp rate: of 4 °C/mim	stress
3rd step	Unloading	Temp: T_{tr}−20 °C	strain
4th step	Heating	Zero load Temp rate: 4 °C/mim	strain

Results and Discussion

Characterization Results of the SMPs

The thermo-mechanical characterization of SMP 'A' was performed using the rectangular specimens in the bending mode and illustrated in Figure 3. Note that the numbers inside the plot windows indicates the testing step in Figure 1. For this small strain case, the linear relationship as expected was observed between stress and strain at the first step of the thermo-mechanical test. In the second step, the effect of the thermal shrinkage was not clearly observed. Were it involved, the constant strain condition in this step might increase the stress due to the restricted thermal contraction. For the moment, it is not clear why the thermal contraction was not involved. The strain fixity rate in this sample was not higher since about 50 % strain was recovered after the cooling process. This may indicate that in the sample 'A' the hard and soft segments are not separated well, i.e., interconnected. This fact is also confirmed from temperature and strain plot in Figure 3. The strain recovery rate is almost constant and very similar to the modulus at high temperature, indicating that the phase separation is not complete. Note that once the heated sample was deformed, the stiffness in the cooled sample was

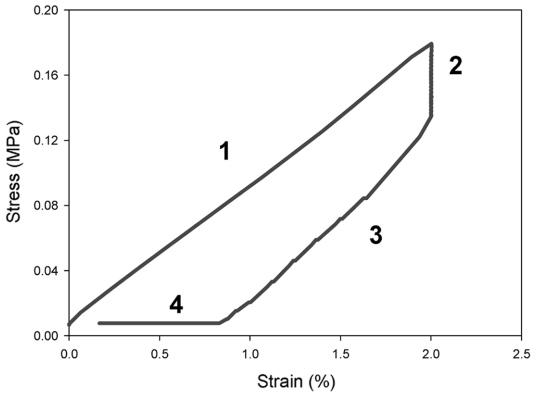

(a)

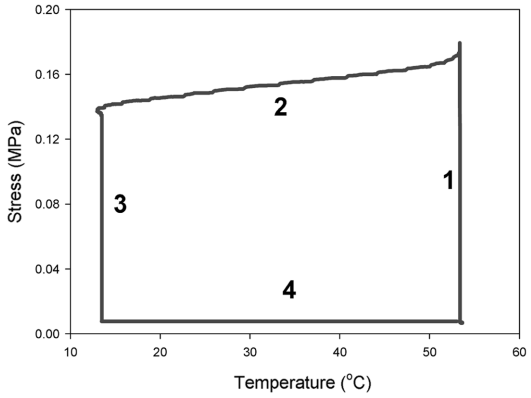

(b)

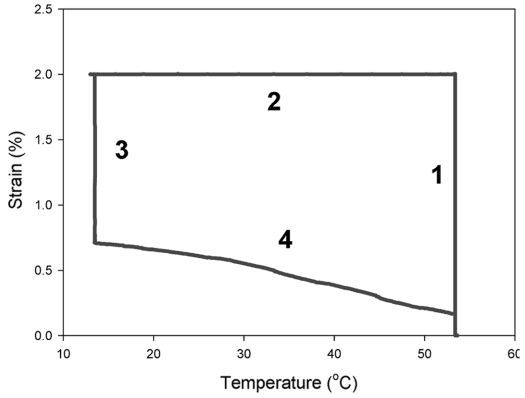

(c)

Figure 3. Thermo-mechanical test result of sample 'A' SMP; (a) stress-strain curve, (b) stress-temperature, and (c) strain-temperature curve.

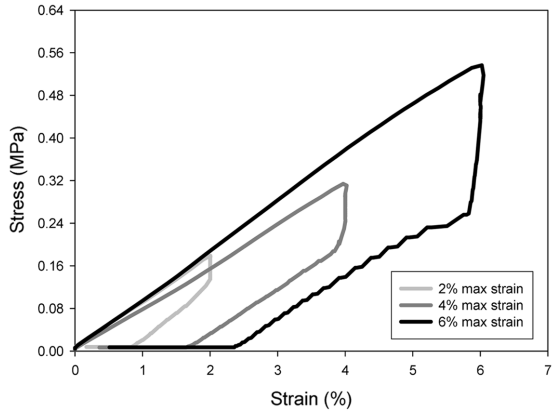

Figure 4. Themomechanical deformation behavior of sample 'A' SMP.

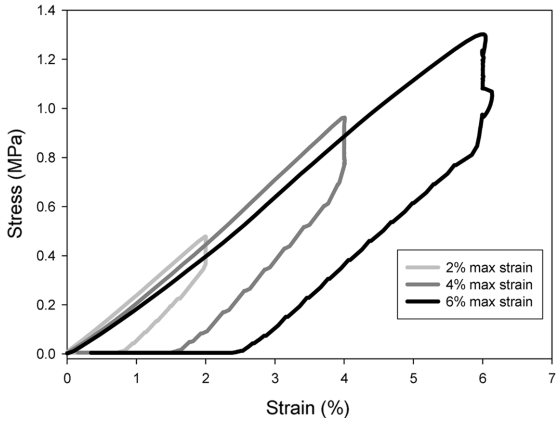

Figure 5. Themomechanical deformation behavior of sample 'B' SMP.

Table 3. Shape memory performance of two SMPs

Sample	ε_m (%)	ε_u (%)	ε_p (%)	R_r^* (%)	R_f^* (%)
A	2	0.7114	0.1667	91.665	35.57
	4	1.434	0.3603	90.9925	35.85
	6	2.0739	0.51	91.5	34.565
B	2	0.5915	0.0477	97.615	29.575
	4	1.2426	0.1554	96.115	31.065
	6	2.0171	0.3454	94.24	33.618

*$R_f = (\varepsilon_u/\varepsilon_m)\times 100$ and $R_r = (\varepsilon_m - \varepsilon_p)/\varepsilon_m \times 100$.

deteriorated in the low temperature. As the maximum strain imposed increases, this tendency remains as shown in Figure 4. For the sample 'B' SMP, the same tendency was observed overall (see Figure 5) but the stiffness was a little different. The latter is more rigid than the former, which may be beneficial to SMP application because high rigidity implies large recovery power for the same strain. The shape memory performance of the two materials is summarized in Table 3.

The thermo-mechanical behavior of the SMP fibers spun from the two SMPs was investigated using the tensile mode in DMTA. Prior to the thermo-mechanical test, the tensile modulus was measured with the constant strain rate, showing that the PCL based SMP (sample 'B') has better tensile properties (see Figure 6). The higher tensile modulus and tenacity indicate that the recovery power is also strong and may be more beneficial to smart fibers. The thermo-mechanical test of the SMP fibers were also carried out, and at this time the maximum strain was increased to 25 %, 50 % and 80 %.

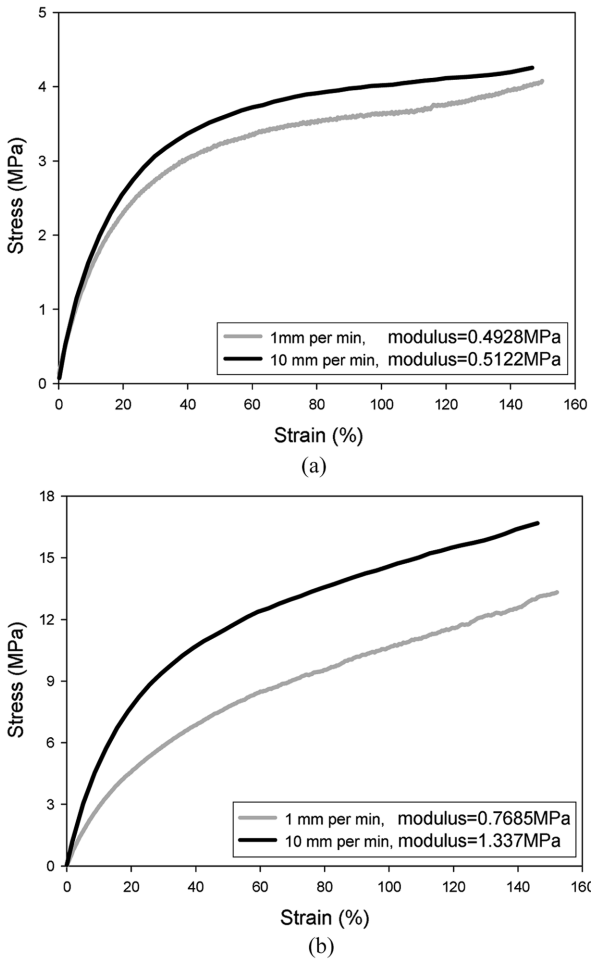

Figure 6. Tensile properties of fibers spun from two SMPs; (a) SMP 'A' fiber (137 denier) and (b) SMP 'B' fiber (180 denier)

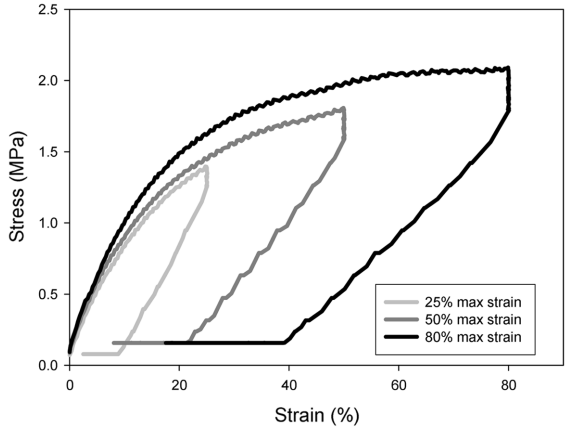

Figure 7. Thermo-mechanical behavior of smart fibers spun from sample 'A' SMP.

As shown in Figure 7 and 8, the hysterisis becomes more pronounced as the maximum strain increases. The nonlinear behavior was also observed for this large deformation case.

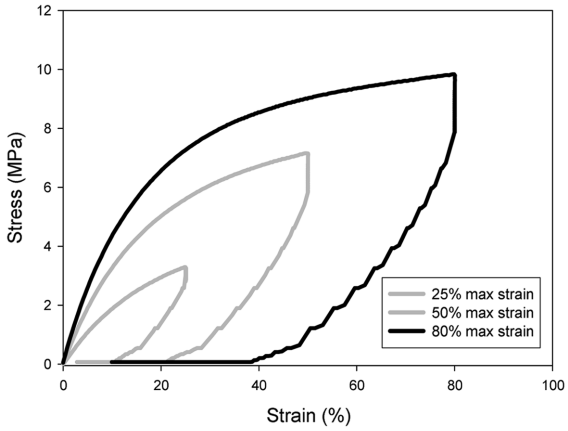

Figure 8. Thermo-mechanical behavior of smart fiber spun from sample 'B' SMP.

Note that the shape memory performance such as the strain fixity and recovery rates are very similar to the small deformation case, implying that strain hardening/softening mechanism was not involved significantly in these two SMPs.

Constitutive Modelling of SMP

To describe the 'frozen' stress and its 'activation' in SMP, the linear viscoelastic theory was applied as the first trial. Since the 'linear' theory implies its limitation to the small deformation, we focus on the description of thermo-mechanical behavior of SMPs within the small deformation range. For the large deformation case (see the experimental for the shape memory fibers), a nonlinear viscoelastic model will be adopted and reported in a future elsewhere.

The linear viscoelastic theory can be described by the hereditary integral derived by Boltzmann superposition principle as follows.

$$\sigma(t) = \int_{-\infty}^{t} E(t-s)\frac{d\varepsilon}{ds}ds \tag{1}$$

where σ, ε, and E are stress, strain, and the relaxation modulus, respectively. Equation (1) can be used to calculate the stress at the constant temperature, provided that the relaxation modulus and strain history are specified. To describe temperature varying deformation behavior of SMP, equation (1) needed to be modified to:

$$\sigma(t) = \int_{-\infty}^{t} E(\xi-\xi')\frac{d\varepsilon}{ds}ds \tag{2}$$

where ξ and ξ' are the reduced (or intrinsic) times [23] as defined below, respectively.

$$\xi = \int_{-\infty}^{t}\frac{d\tau}{a_T(\tau)}, \quad \xi' = \int_{-\infty}^{s}\frac{d\tau}{a_T(\tau)} \tag{3}$$

Here, a_T is the shift factor which can be determined by shifting the relaxation curve at a temperature to the reference temperature.

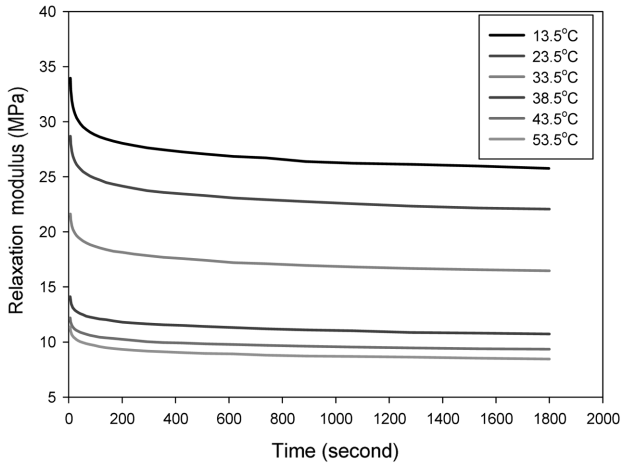

Figure 9. Relaxation modulus curve of shape memory polymer at various temperatures.

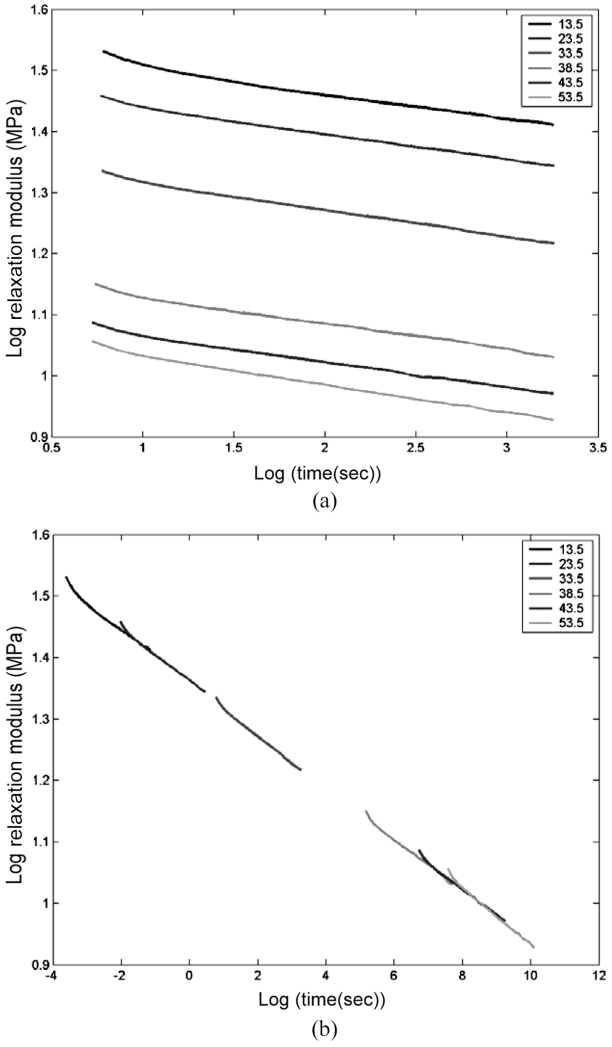

Figure 10. Log-log plot of (a) stress relaxation curve and (b) the shifted relaxation curve.

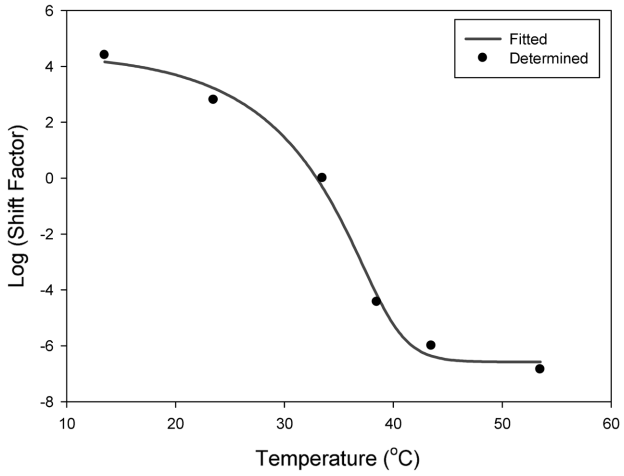

Figure 11. Determined shift factor by horizontally translating the relaxation curve.

For the thermo-mechanical description of SMP, the relaxation modulus was measured for sample 'A' by varying the temperature from 13.5 to 53.5 °C as shown in Figure 9. A constant strain of 3 % was applied for 30 minutes for this relaxation test. It is observed that the relaxation time becomes shorten as the temperature increases. The master curve of the relaxation modulus was obtained at a reference temperature (here, T_{tr}=33.5 °C) by calculating the shift factor, which was determined using the conventional method by plotting the relaxation curve in log time and log modulus axis as shown in Figure 10. Then, the shift factor (see Figure 11) was used for the calculation of the reduced time under the varying temperature condition. Finally the relaxation curve at the reference temperature was determined in the exponential form as follows (see Table 4 for the coefficients and Figure 12 for the master curve).

$$E = \sum_{i=1} E_i \exp(-t/\tau_i) \tag{5}$$

It was assumed that SMPs are 'thermo-rheologically simple material'. To validate this assumption, the relaxation curves in Figure 9 were calculated using the master curve, the shift factor, and equation (2), demonstrating that the 'thermo-rheologically simple material' assumption for SMP is acceptable as shown in Figure 13. The initial part of each relaxation curve, however, was not predicted very well, which may be due to the deviation of the initial part from the shifted master curve (see Figure 10(b)).

Simulation of the Thermo-mechanical Deformation Behavior of SMP

Temperature varying properties can be modelled using the master curve and shift factor as explained in the previous section. Using these information and equation (2), the thermo-mechanical deformation behavior of SMPs can be simulated. In

Table 4. Relaxation time spectrum

i	0	1	2	3	4	5	6	7	8
$1/\tau_i$(s)	0	2.021×10^{-3}	6.029×10^{-2}	279.6	1.137	16.39	4.274×10^{-6}	3724	1.493×10^{-8}
E_i(MPa)	9.393	2.786	3.253	3.179	2.55	3.004	4.154	7.027	2.857

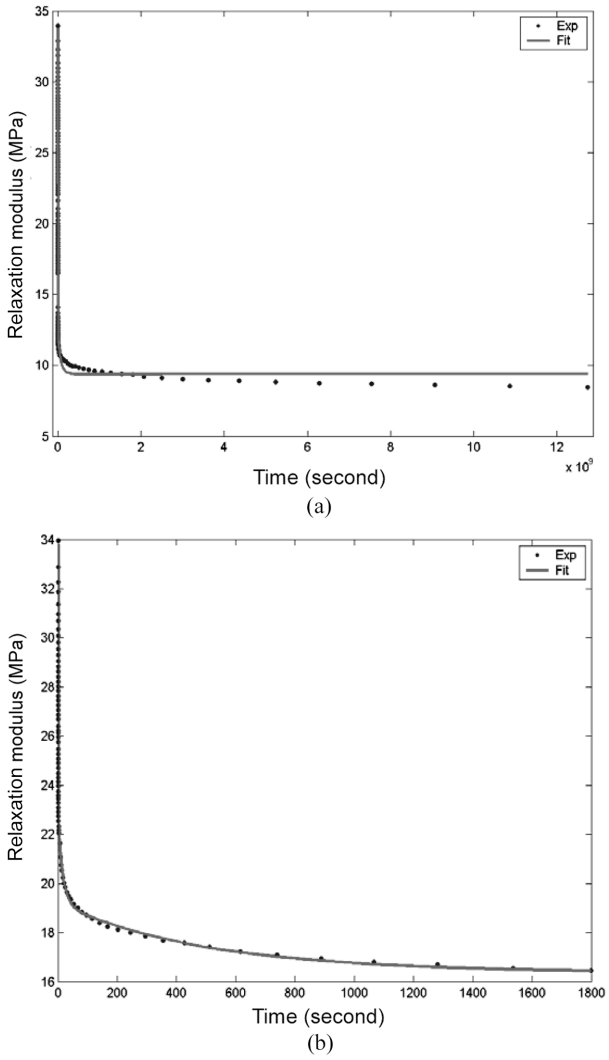

Figure 12. Master relaxation curve at the reference temperature; (a) 0 to 12×10^9 seconds and (b) 0 to 1800 seconds.

this simulation, it was assumed that the stress in equation (2) is generated by the mechanical strain only, which can be obtained by subtracting the thermal strain from the total strain. For the thermal strain calculation, the thermal expansion/contraction coefficient (11.6E-5 (/K)) was adopted from the literature [19].

Figure 14 shows the simulation result of thermo-mechanical behaviour of SMP. The linear strain-stress behavior was predicted in the first step of the thermo-mechanical test, which is consistent with the experiment. The second step in this simulation does not show the increase of the stress, due

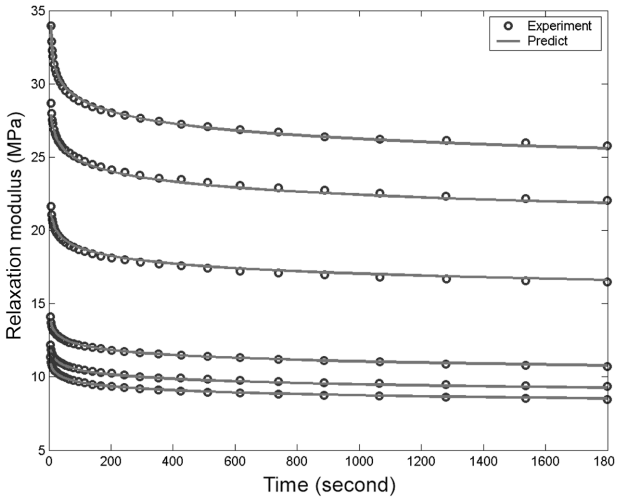

Figure 13. Validation of thermo-rheologically simple material assumption for a shape memory polymer.

to the small thermal strain involved. In the experiment, the stress was not relaxed quickly than in the simulation, deducing that the master curve for the relaxation modulus at the reference temperature may not be accurate enough to describe the temperature varying relaxation modulus. As the temperature increases after the second and third step (the fixation step of the strain), the strain recovery process expedites. Note that the strain recovery is not linear (see Figure 14) with the increased temperature, instead it increases significantly at the high temperature beyond the transition one. This result is consistent with the relaxation curve in Figure 9, i.e., the relaxation modulus drops significantly in the high temperature beyond the transition temperature. In conclusion, the linear viscoelastic model seems to describe the thermo-mechanical behavior of SMP such as the strain fixity and recovery rate; however, in the third step the simulation result is not comparable with experiment (see the third step in Figure 3(a) and Figure 14(a)), the reason of which should be discussed as follows.

The relaxation modulus in Figure 9 shows about three order difference in modulus between T_l(=13.5 °C) and T_h (=53.5 °C). The huge difference brings out different paths in the stress and strain relationship according to the temperature, i.e., the slope of stress and strain at T_h is smaller than one at T_l, imparting the strain fixity and recovery properties to SMP. This consideration can be also confirmed by theoretical simulation in Figure 14. On the contrary, the thermo-mechanical test in Figure 4 through Figure 5 does not reflect the huge difference in modulus T_l and T_h, making it possible to deduce other mechanism involved by the thermal treatment.

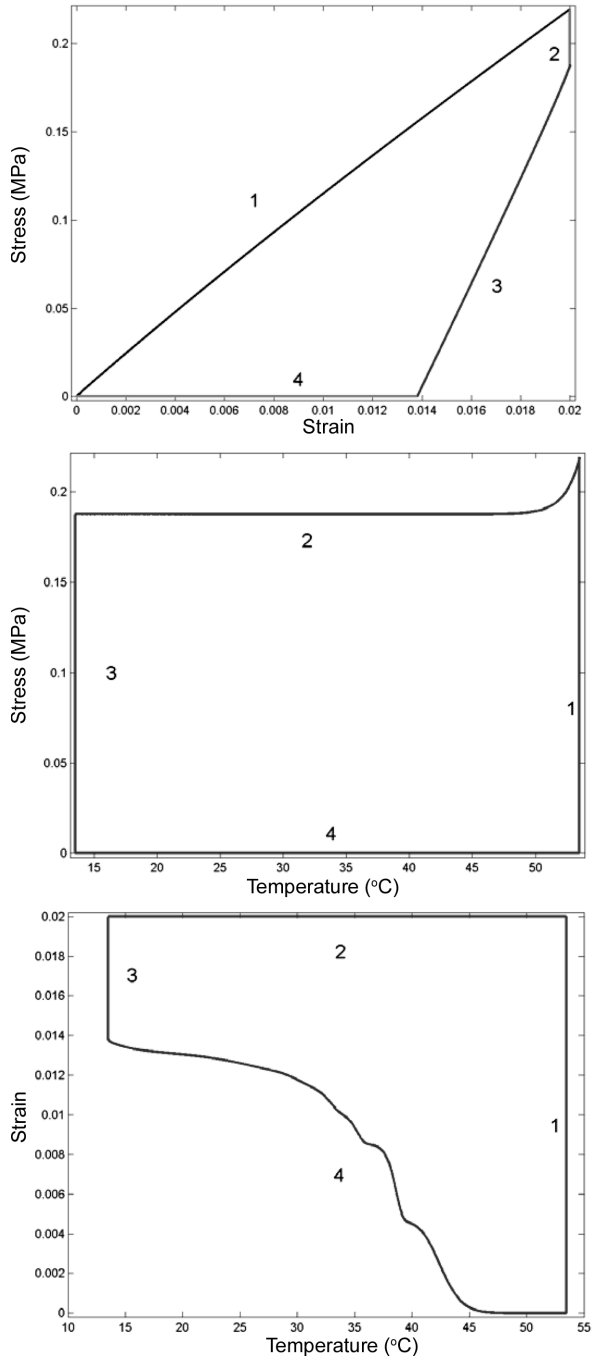

Figure 14. Thermo-mechanical simulation results (top: strain-stress relationship, middle: temperature-stress relationship, bottom: temperature-strain relationship).

Therefore, the following experiments were performed with SMP 'A' material (sample dimension: 10 mm×3 mm×1 mm).

Three experiments were carried out. Firstly, at T_l the sample was strained to 3 % with a strain rate of 2 mm/min. Then, the sample was returned with the same strain rate to the undeformed configuration, followed by 8 times repeated testing. The second experiment was also the repeated tensile

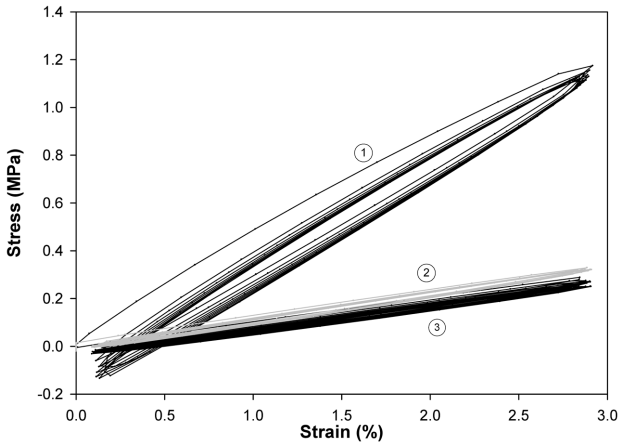

Figure 15. Comparison of the cyclic tensile test of SMP; ①: cyclic tensile test at T_l(=13.5 °C), ②: cyclic tensile test at T_l(=13.5 °C) after the thermal treatment at T_h(=53.5 °C), and ③: cyclic tensile test at T_h(=53.5 °C).

test but different thermal history. The sample was first heated to T_h and left for one minute, followed by cooling to T_l. Then, again at T_l, the same cyclic tensile test was applied. Thirdly, the same tensile test was carried out at T_h. Two noticeable points can be observed from these experiments as shown in Figure 15. One point is the consistent mechanical behavior of SMP in the cyclic loading, which are true for all the three experiment conditions. The other point is that the thermal treatment seems to change significantly the micro-structure in the current SMP. After the thermal treatment at T_h, the tensile behavior of SMP, which was already cooled down to T_l, became similar to the one at the high temperature (compare ② and ③ in Figure 1). This deteriorated rigidity after the thermal treatment lowers the strain fixity rate of SMP. In conclusion, the current SMPs used in this study seem not phase-separated enough to reveal high shape memory performance. In the mechanical modelling using the linear viscoelastic theory, this reduced rigidity due to the thermal treatment was not considered so that the discrepancy between experiment and theory was not avoidable.

Conclusion

PU SMPs were spun into fibers using the conventional extrusion technology to investigate the feasibility of making smart fibers with shape memory function using them. The thermo-mechanical behavior of the SMPs and their fibers were characterized using DMTA. For the small deformation, the bending mode was utilized to characterize SMP using the film specimen, whereas the tensile mode was adopted for the fibers, in particular large deformation characterization. It was observed that the fibers spun from the SMPs behaved in the same way as their bulk form did, thereby suggesting that the smart fibers with the smart functions such as the strain

fixity and recovery properties according to temperature can be manufactured from SMP.

To model the thermo-mechanical behavior of SMP, the linear viscoelastic theory was applied using the time-temperature supposition and the reduced time concept. It was found that in general the linear viscoelastic model can predict the characteristics of SMPs, in particular the strain fixity and recovery properties in the small deformation regime, however discrepancy between experiment and calculation was observed. A main source for this error was found to the reduced rigidity of SMP due to the thermal treatment, which should be avoided for better shape memory performance of SMPs.

Acknowledgement

The authors of this paper would like to thank the Korea Science and Engineering Foundation (KOSEF) for sponsoring this research through the SRC/ERC Program of MOST/ KOSEF (R11-2005-065). This work is also partly supported by Ministry of Commerce, Industry, and Energy in Korea for which the authors feel grateful.

References

1. A. Lendlein and S. Kelch, *Angew. Chem. Int. Ed.*, **41**(12), 2034 (2002).
2. H. Tobushi, H. Hashimoto, and N. Ito, *J. Intel. Mat. Syst. Str.*, **9**(2), 127 (1998).
3. X. L. Meng, Y. F. Zheng, Z. Wang, and L. C. Zhao, *Mater. Lett.,* **45**(2), 128 (2000).
4. H. M. Wache, D. J. Tartakowska, A. Hentrich, and M. H. Wagner, *J. Mater. Sci.-Mater. M,* **14**(2), 109 (2003).
5. A. Lendleing and R. Langer, *Science*, **296**(5573), 1673 (2002).
6. N. M. K. Lambe, K. A. Woodhouse, and S. L. Cooper, "Polyurethanes in Biomedical Applications", CRC Press, 1998.
7. J. W. Cho, Y. C. Jung, Y.-C. Chung, and B. C. Chun, *J. Appl. Polym. Sci.*, **93**(5), 2410 (2004).
8. B. K. Kim, S. Y. Lee, and M. Xu, *Polymer*, **37**(26), 5781 (1996).
9. B. K. Kim, S. Y. Lee, J. S. Lee, S. H. Baek, Y. J. Choik, J. O. Lee, and M. Xu, *Polymer*, **39**(13), 2803 (1998).
10. B. K. Kim, Y. J. Shin, S. M. Cho, and H. M. Jeong, *J. Polym. Sci. Pol. Phys.*, **38**(20), 2652 (2000).
11. J. R. Lin and L. W. Chen, *J. Appl. Polym. Sci.*, **69**(8), 1575 (1998).
12. F. Li, X. Zhang, J. Hou, M. Xu, X. Luo, D. Ma, and B. K. Kim, *J. Appl. Polym. Sci.*, **64**(8), 1511 (1997).
13. H. Tobushi, H. Hara, E. Yamada, and S. Hayashi, *Smart. Mater. Struct.*, **5**(4), 483 (1996).
14. Y. S. Shim, B. C. Chun, and Y.-C. Chung, *Fibers and Polymers*, **7**(4), 328 (2006).
15. K. Gall, M. L. Dunn, Y. Liu, D. Finch, M. Lake, and N. A. Munshi, *Acta Mater.*, **50**(20), 5115 (2002).
16. V. A. Beloshenko, Y. E. Beigelzimer, A. P. Borzenko, and V. N. Varyukhin, *Mech. Compos. Mater.*, **39**(3), 255 (2003).
17. H. Hosoda, S. Takeuchi, T. Inamura, and K. Wakashima, *Sci. Tech. Adv. Mater.*, **5**(4), 503 (2004).
18. J. M. Hampikian, B. C. Heaton, F. C. Tong, Z. Zhang, and C. P. Wong, *Mat. Sci. Eng. C: Biomimetic Supramol. Syst.*, **26**(8), 1373 (2006).
19. H. Tobushi, T. Hashimoto, S. Hayashi, and E. Yamada, *J. Intel. Mat. Syst. Str.*, **8**, 711 (1997).
20. H. Tobushi, K. Okumura, S. Hayashi, and N. Ito, *Mech. Mater.*, **33**, 545 (2001).
21. Y. Liu, K. Gall, M. L. Dunn, A. R. Greenberg, and J. D. Diani, *Int. J. Plasticity*, **22**, 279 (2006).
22. P. Ping, W. Wang, X. Chen, and X. Jing, *Biomacromolecules*, **6**, 587 (2005).
23. L. W. Morland and E. H. Lee, *Trans. Soc. Rheol.*, **4**, 233 (1960).